Energy Transfer within Zn-Porphyrin Dendrimers: Study of the Singlet−Singlet Annihilation Kinetics

Jane Larsen,* Ben Brüggemann, Tomáš Polívka,† Villy Sundström, and Eva Åkesson

Department of Chemical Physics, Lund University, Box 124, SE-221 00 Lund, Sweden

Joseph Sly‡ and Maxwell J. Crossley

School of Chemistry, The University of Sydney, NSW 2006, Australia

Received: June 28, 2005; In Final Form: September 23, 2005

In this article, we explore energy transfer processes within a series of Zn-porphyrin-appended dendrimers by means of excitation intensity dependent transient absorption measurements. We report singlet−singlet annihilation on two distinct time scales of 18 ± 5 ps and 130 ± 10 ps in the dimer and the dendrimers. The two distinct processes reflect the presence of two structural conformer distributions. Analysis of the singlet−singlet annihilation transient kinetics shows that sequential annihilation occurs within subunits up to four Zn-porphyrins in the dendrimers. The onset of the singlet−singlet annihilation process depending on the size of the molecule reveals a difference in the number of communicating Zn-porphyrins. We further report a full characterization of the transient absorption kinetics of the monomer over a spectral range from 450 to 730 nm.

1. Introduction

Dendrimers are characterized by a highly branched symmetric structure. The high degree of symmetry often allows for a precise description of these large macromolecules based on the properties of a monomer. Dendrimers have been suggested for many applications including guest−host chemistry,[1] analytical chemistry,[2] optical data storage,[3,4] catalytic chemistry,[5] environmental chemistry,[6,7] biology,[8−13] and medical applications.[14] In addition, dendrimers have been proposed as light-harvesting (LH) antennas in artificial photosynthesis due to their capability of directional energy transfer (ET) within the dendrimers.[15−30]

In natural LH systems, (bacterio)chlorophyll pigments are arranged in well-defined positions usually on or near the surface of a three-dimensional shape. In the case of photosystems I and II the pigments lie in the outer regions of an ellipsoid,[31,32] while the chromophores of the LH units, LH1 and LH2, in purple bacteria are arranged on the outer periphery of a torus.[33,34] The number of LH pigments used depends on the system and varies from 7 in the FMO complex of green sulfur bacteria[35,36] to 96 in the photosystem I complex of the cyanobacterium *Synechococcus elongatus*.[32] ET between the (bacterio)chlorophylls (BChl's) in, for example, the LH ring systems in purple bacteria occurs on a time scale ranging from subpicoseconds to tens of picoseconds.[37] However, BChl's cannot be utilized in artificial antenna systems due to their low chemical stability. The porphyrin-appended dendrimers used in this investigation offer a more stable alternative to BChl, and furthermore mimic the structural aspect of the natural photosystems in that the Zn-porphyrins are attached to the exterior of the dendrimers and the number of pigments ranges from 4 to 64. The pigments of the natural systems are located at more or less fixed positions within each antenna unit. In the porphyrin-appended dendrimers used in this study, there is greater conformational freedom because of the flexibility of the single bond network of the dendrimer core. It is of interest to determine the effect of this flexibility on the energy transfer (ET) processes that occur within these porphyrin-appended dendrimers because it should increase understanding of the reasons that Nature has evolved LH antenna with relatively rigid and very well-defined pigment arrays.

ET within dendrimers is frequently well described by Förster ET theory. This has previously been reported in polyphenylene dendrimers,[24−28] free-base porphyrin dendrimers,[29] self-assembled Zn-porphyrin tetramer,[30] and bis-porphyrins with quinoxaline Tröger's base and biquinoxalinyl spacers.[38] To measure ET within the dendrimers, time-resolved anisotropy experiments have regularly been utilized.[27−30,38,39] As an alternative to anisotropy measurements, excitation intensity dependent measurements can provide valuable information about the ET. This method has been applied to dendrimers[19,40,41] as well as to photosynthetic antenna systems such as LH2.[42−44] Increasing the excitation intensity will increase the possibility of singlet−singlet annihilation within the chromophore complex.

$$S^* + S^* \xrightarrow{ET} S + S^{**} \xrightarrow{\text{fast nonradiative decay}} S + S^*$$

The first step in singlet−singlet annihilation is ET between two excited chromophores. This results in a deexcitation of one chromophore to the ground state along with a double excitation of the other chromophore followed by fast nonradiative decay to the lowest excited state. Often, the ET process is well described by Förster ET theory, which requires a spectral overlap between the emission spectrum of the donor and the excited state absorption spectrum of the acceptor. Mathematically the singlet−singlet annihilation process can be expressed as[45,46]

* Corresponding author. E-mail: Jane.Larsen@chemphys.lu.se.

† Current address: Institute of Physical Biology, University of South Bohemia, Zamek 136, CZ-373 33 Nove Hrady, Czech Republic.

‡ Current address: IBM Almaden Research Center, 650 Harry Road, San Jose, CA 95120.

10.1021/jp053514z CCC: $30.25
Published on Web 11/08/2005

$$\frac{dn}{dt} = -kn(t) - \gamma(t)\, n(t)^2 \quad (1)$$

where n is the population of the excited state, $n(t=0) = n_0$, and k is the decay rate of the excited state. In large aggregates with a high mobility of excitons, the annihilation rate constant, $\gamma(t)$, can be assumed to be time-independent and the solution to eq 1 yields

$$n(t) = \frac{n_0 \exp(-kt)}{1 + n_0 \gamma k^{-1}[1 - \exp(-kt)]} \quad (2)$$

However, the annihilation dynamics observed in the Zn-porphyrin dendrimers reported in this article do not follow eq 2, and a more general approach also valid for small aggregates is needed. This can be achieved by using a time-dependent annihilation rate constant $\gamma(t)$.[47] We have chosen a rate equation approach because of its flexibility. One can easily include the intersystem crossing (ISC) to the triplet state and more than one annihilation rate, both of which are needed for a proper description of the measured data.

2. Material and Methods

2.1. Theory. The statistical approach using rate equations cares for the dynamics of each number of excitons separately.[47] For other systems where the number of highly mobile excitons is much larger, the chosen rate equation approach will reduce to eqs 1 and 2 upon calculating the average number of excitons.[47] Here we will use a simplified version of this approach. Considering only two chromophores, we use rate equations for the number of Zn-porphyrins in the singlet state (S) and the triplet state (T), and additionally for the number of exciton pairs, which annihilate due to singlet−singlet annihilation. The chosen approach is also valid for larger numbers of chromophores, if any of them can only once be involved in an annihilation process. The Zn-porphyrin compounds are very flexible.[48,49] Furthermore, the annihilation rate is strongly dependent on the distance between the Zn-porphyrins and the orientation of the dipole moments. This makes it reasonable that more than one annihilation rate constant can be observed, even in the example of only two chromophores. Assuming that the annihilation can be divided into a fast (f) and a slow (s) process, the change in the number of exciton pairs responsible for each process is given by

$$\frac{dE_M}{dt} = -k_M E_M(t) \quad (3)$$

where E_M is the number of the exciton pairs related to either the fast (M = f) or the slow (M = s) annihilation process with $E_M(t=0) = E_{M0}$. The corresponding annihilation rate constants k_M include the Förster ET to doubly excite one chromophore and deexcite the other, and the following fast internal conversion process within the first chromophore. Note that internal conversion, ISC, and radiative decay to the ground state are not included in eq 3, since it only describes the exciton pairs that annihilate. The decay of the singlet state (S) and the buildup of the triplet state (T) are given by

$$\frac{dS}{dt} = -kS(t) + k_f E_f(t) + k_s E_s(t) \quad (4)$$

and

$$\frac{dT}{dt} = k_{ISC} S(t) - k_T T(t) \quad (5)$$

where k is the sum of the radiative decay rate (k_r), the internal conversion rate (k_{IC}), and the ISC rate to triplet states (k_{ISC}), $S(t=0) = S_0$ and $T(t=0) = 0$. The decay of the triplet state $k_T \ll k_{ISC}$, and is therefore set to zero.

The observed transient signal at a given probe wavelength, where ground state bleaching and stimulated emission are not present, can be described by

$$\Delta A(t) = S(t) + pT(t) + 2E_f(t) + 2E_s(t) \quad (6)$$

The annihilation amplitudes contribute twice since they each describe a pair of excitons. p is the ratio between the extinction coefficient of the singlet excited transition and the triplet transition at the selected probe wavelength. The solutions to eqs 3−5 inserted in eq 6 yields

$$\Delta A(t) = A_0 + A_1 \exp(-kt) + A_2 \exp(-k_s t) + A_3 \exp(-k_f t) \quad (7)$$

where

$$A_0 = \frac{pk_{ISC}}{k}[S_0 + E_{s0} + E_{f0}] \quad (8)$$

$$A_1 = \left(1 - \frac{pk_{ISC}}{k}\right)\left[S_0 + \frac{k_f}{k_f - k}E_{f0} + \frac{k_s}{k_s - k}E_{s0}\right] \quad (9)$$

$$A_2 = \left[1 + \frac{k - pk_{ISC}}{k - k_s}\right]E_{s0} \quad (10)$$

and

$$A_3 = \left[1 + \frac{k - pk_{ISC}}{k - k_f}\right]E_{f0} \quad (11)$$

The transient absorption signals can therefore be reproduced by a triple-exponential decay function.

2.2. Experimental Procedures. Steady state absorption spectra were measured on a UV/vis dual-beam spectrophotometer. Fluorescence steady state spectra were measured on a Spex Fluorolog II with a spectral resolution of 0.5 nm, detected with a photomultiplier tube (PMT) and corrected afterward for the wavelength dependent PMT sensitivity.

Transient absorption measurements were performed with the output from a 1 kHz Ti:sapphire laser amplified by the second harmonic of a Nd:YLF laser (both from Spectra Physics). The majority of the 836 nm output from the amplified laser was frequency doubled in a BBO crystal to yield 418 nm used as excitation light. The polarization of the excitation light was set to 54.7° (magic angle) with respect to the polarization of the probe light using a Berek polarizer compensator. Different neutral density filters were inserted before the sample to vary the intensity of the excitation light from 4×10^{14} to 1.6×10^{17} photons/cm^2 per pulse.

The residual of the amplified laser output beam was focused into a 0.5 mm sapphire plate to generate white light continuum used for probing. The probe light was divided into a reference beam and a probe beam, the latter overlapping the pump beam in a 2 mm rotational quartz cuvette at an angle of ~15°. Two diode arrays were used to detect the probe and reference light in the spectral range from 450 to 730 nm. The time resolution in the experiments was ~150 fs.

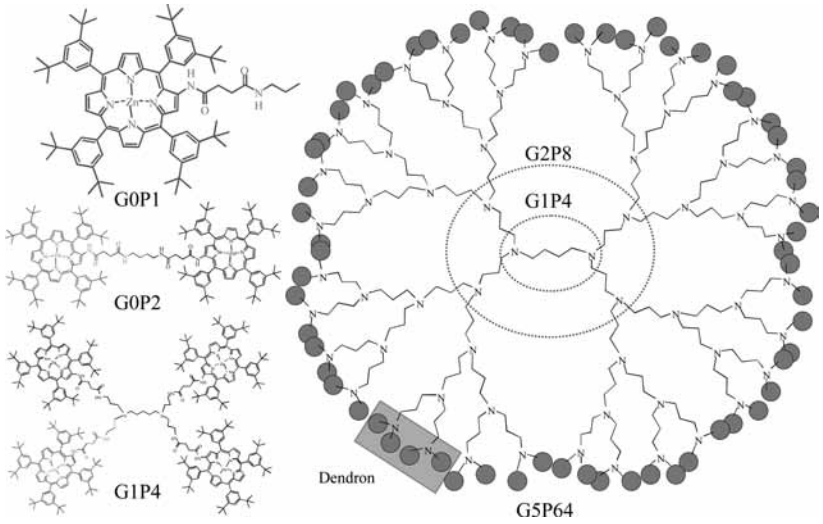

Figure 1. Structure of the Zn-porphyrin compounds. In the left column, the monomer (G0P1), the dimer (G0P2), and the first generation dendrimer (G1P4) are displayed, whereas the largest dendrimer, the fifth generation (G5P64), is shown to the right. The monomer is marked with gray in G0P2 and G1P4 and is illustrated with the gray circles in G5P64. The two dotted ellipses in G5P64 show where the monomers are attached for the first and second generations. The gray square in G5P64 marks a unit of four Zn-porphyrins, also referred to as a dendron.

Nanosecond flash photolysis was employed to measure the triplet spectrum. The samples were excited at 600 nm (lowest energy Q-band) with 8 ns pulses from a Quanta-Ray Master Optical Parametric Oscillator (MOPO) pumped by a 355 nm Quanta-Ray 230 Nd:YAG laser (Spectra Physics). A 75 W Xe-arc lamp provided the white light probe, which was spectrally filtered by a monochromator and detected afterward by a PMT. The pump and the probe light overlapped collinearly in the 1 cm quartz cuvette. All flash photolysis traces were recorded in a 10 μs time window.

The synthesis and purification of the compounds have been described previously.[50] Before use, the compounds were dissolved in tetrahydrofuran (THF) purchased from Merck. The solvent was degassed with nitrogen and used without further purification. The optical density at 430 nm was 0.1 mm^{-1} in the steady state absorption experiments, less than 0.01 mm^{-1} in the steady state fluorescence experiments, and 0.8−1.4 mm^{-1} in the time-resolved experiments. This yields concentrations of $10^{-7}-10^{-5}$ M in the time-resolved experiments, with the highest generation dendrimer having the lowest concentration. The cross section at 429 nm is 0.225×10^{-14}, 4.45×10^{-14}, 8.36×10^{-14}, 15.9×10^{-14}, and 118×10^{-14} cm^2/molecule for G0P1, G0P2, G1P4, G2P8, and G5P64, respectively.[49] Fresh samples were prepared prior to each measurement to avoid degradation of the samples. Steady state absorption spectra measured before and after each measurement showed no sign of degradation for excitation intensities below 10^{17} photons/cm^2 per pulse. The data have been corrected for sample degradation observed above excitation intensities of 10^{17} photons/cm^2 per pulse.

3. Results

3.1. Structural and Spectral Characteristics of the Compounds. The dendrimers are constructed from a single-bonded nitrogen and carbon skeleton. Monomeric Zn-porphyrins (G0P1) are attached at the end of each skeleton arm. This is illustrated in Figure 1 for the first generation dendrimer with four Zn-porphyrins (G1P4). By expanding the skeleton, higher orders of dendrimers are obtained. In addition to the first generation dendrimer, the second and the fifth generations with 8 and 64 Zn-porphyrins, respectively, are used in the experiments presented here. As a reference, measurements are also performed on the monomer and the dimer (G0P2). In Figure 1, the gray circles at the ends of the G5P64 arms symbolize one monomer. The dotted ellipses in G5P64 mark the positions of the Zn-porphyrins in G1P4 and G2P8. Due to the very flexible single-bonded skeleton, the fifth generation dendrimer resembles a three-dimensional sphere rather than a two-dimensional disk.[29] Earlier time-resolved fluorescence anisotropy measurements have demonstrated a high degree of flexibility, as the rotational motion of the Zn-porphyrins within the dendrimers was comparable to that of G0P1.[49] The Zn-porphyrins are situated on the surface of the spheres, since they are too large for back-folding due to the bulky end groups.[29,50]

Normalized steady state absorption and fluorescence spectra of all the compounds are displayed in Figure 2. The absorption spectra show no variation depending on the dendrimer size, except an increase in extinction coefficient that scales almost linearly with the number of Zn-porphyrins.[49,50] The strongly absorbing Soret band centered at 429 nm corresponds to the $S_2 \leftarrow S_0$ transition, whereas the two much weaker Q-bands shown in the inset correspond to the $S_1[1] \leftarrow S_0[0]$ and $S_1[0] \leftarrow S_0[0]$ transitions observed at 558 and 598 nm, respectively. Fluorescence from the S_1 state is detected at 602 and 655 nm corresponding to the $S_1[0] \rightarrow S_0[0]$ and $S_1[0] \rightarrow S_0[1]$ transitions, respectively. A minor increase in the second fluorescence band relative to the first is seen as the dendrimer size increases. No spectral shift is observed depending on the dendrimer size. The similarities in the steady state spectra of the different compounds indicate that there are no strong interactions between the Zn-porphyrins.

In addition to the S_1 fluorescence, there is an efficient ISC from the S_1 state to the T_3 state with a yield of ~84%.[51] After fast IC to the lowest triplet state, phosphorescence to the ground state can be observed at wavelengths above 800 nm.[51]

3.2. Transient Absorption Spectrum of the Monomer. The transient absorption spectra of the G0P1 measured 5 and 350 ps after excitation at 418 nm with an excitation intensity of 125×10^{14} photons/cm^2 per pulse is shown in Figure 3A. Transient absorption spectra of G0P2−G5P64 measured at low excitation intensities exhibited spectral features similar to those of the monomeric spectrum. This is illustrated in Figure 3B, which shows the transient spectra of G0P1 and G5P64 5 ps after excitation. Hence, G0P1 can be used as a model to describe the dynamics in G0P2 and the higher order dendrimers. The

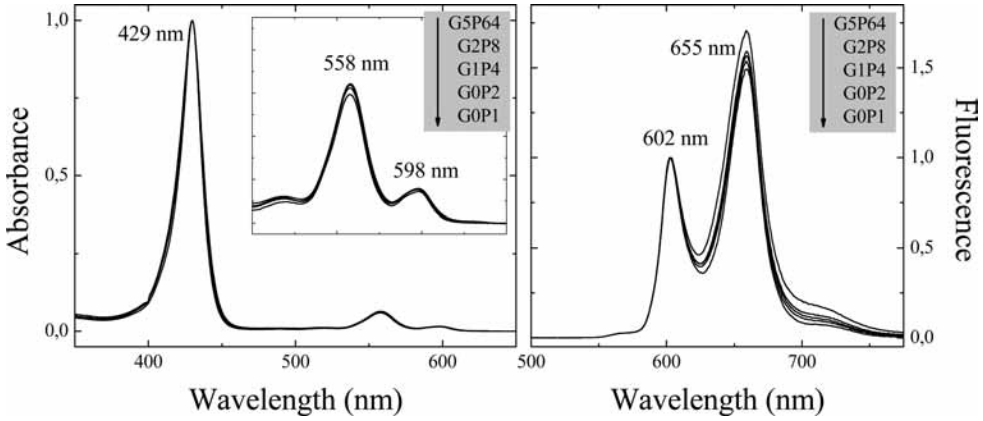

Figure 2. Steady state absorption (left) and fluorescence (right) spectra of the compounds. The absorption spectra are normalized at 429 nm, whereas the fluorescence spectra recorded with exaction at 430 nm are normalized at 602 nm.

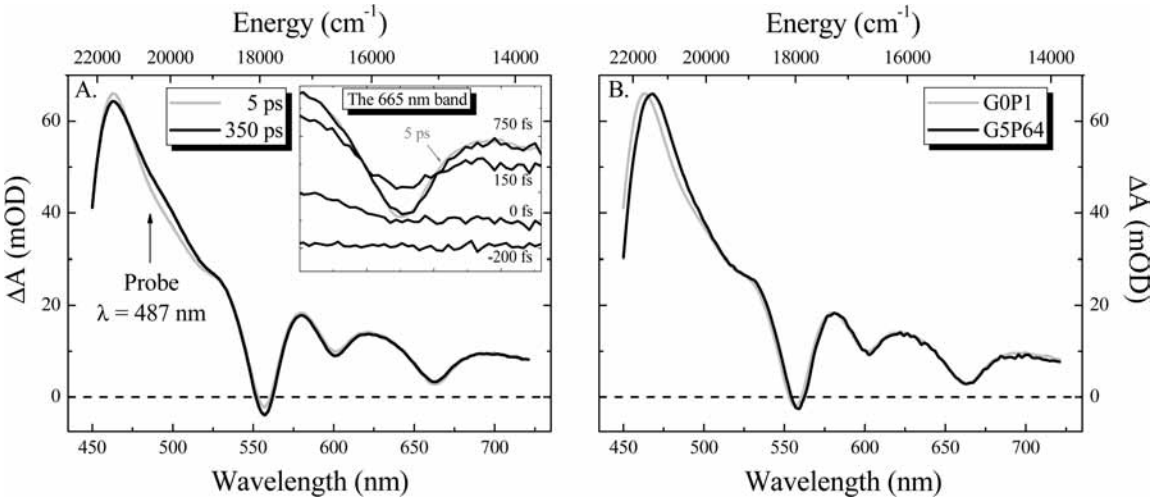

Figure 3. (A) Transient absorption spectrum of GoP1 measured at 5 ps (gray line) and 350 ps (black line) after excitation at 418 nm. The inset displays the 665 nm stimulated emission band around $t = 0$, showing that the IC from S_2 to S_1 takes place on a subpicosecond time scale. (B) Transient absorption spectrum of G0P1 (gray line) and G5P64 (black line) measured at 5 ps.

ground state bleaching is clearly observed at approximately 555 nm, whereas the dip at 600 nm is assigned to a combination of ground state bleaching and stimulated emission, with the latter observed at ~665 nm as well. The inset in Figure 3A shows the evolution of the 665 nm stimulated emission band around time zero. We attribute this fast appearance of the band to IC from the S_2 to the S_1 state occurring on the subpicosecond time scale. Hence, contribution from excited state absorption or stimulated emission from the S_2 state after the first picosecond can safely be neglected. The relatively long S_1 lifetime of 2.7 ns[51] implies that the additional strongly absorbing component with a maximum at ~470 nm, observed within less than 1 ps after excitation, can be assigned to the excited state absorption from the S_1 state. Comparison of the spectra measured at 5 and 350 ps reveals another spectral component in the spectral range from 480 to 490 nm. To identify this component, nanosecond flash photolysis measurements were conducted.

The flash photolysis transient absorption spectrum of G2P8 measured 0.5 μs after the excitation pulse is displayed in Figure 4. Similar spectral features are observed for the monomer (not shown here). Contribution from the ground state bleaching can be observed at 430 and 565 nm. The positive band observed in the figure is characterized by a maximum at 480 nm and a relatively flat plateau below 400 nm. The triplet spectrum of a similar compound reported by Rogers et al. exhibits the same spectral characteristics,[51] and the absorption band shown here peaking at 480 nm is consequently identified as the triplet

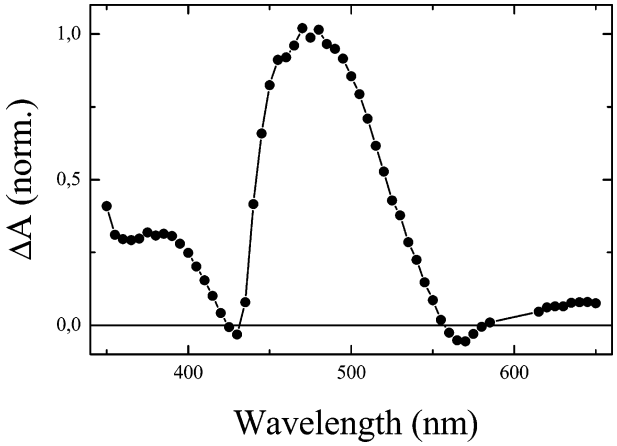

Figure 4. Normalized transient absorption spectrum of G2P8 measured 0.5 μs after excitation at 600 nm. Ground state bleaching is observed at 430 and 665 nm.

spectrum. The additional spectral feature observed at 480−490 nm in the femtosecond transient absorption measurements is thus assigned to the triplet state absorption.

3.3. Excitation Intensity Dependence. When the excitation intensity is increased, the probability of simultaneously exciting more than one Zn-porphyrin within a dendrimer increases and the possibility of singlet−singlet annihilation arises. A decrease of the S_1 population along with an increase of the ground state

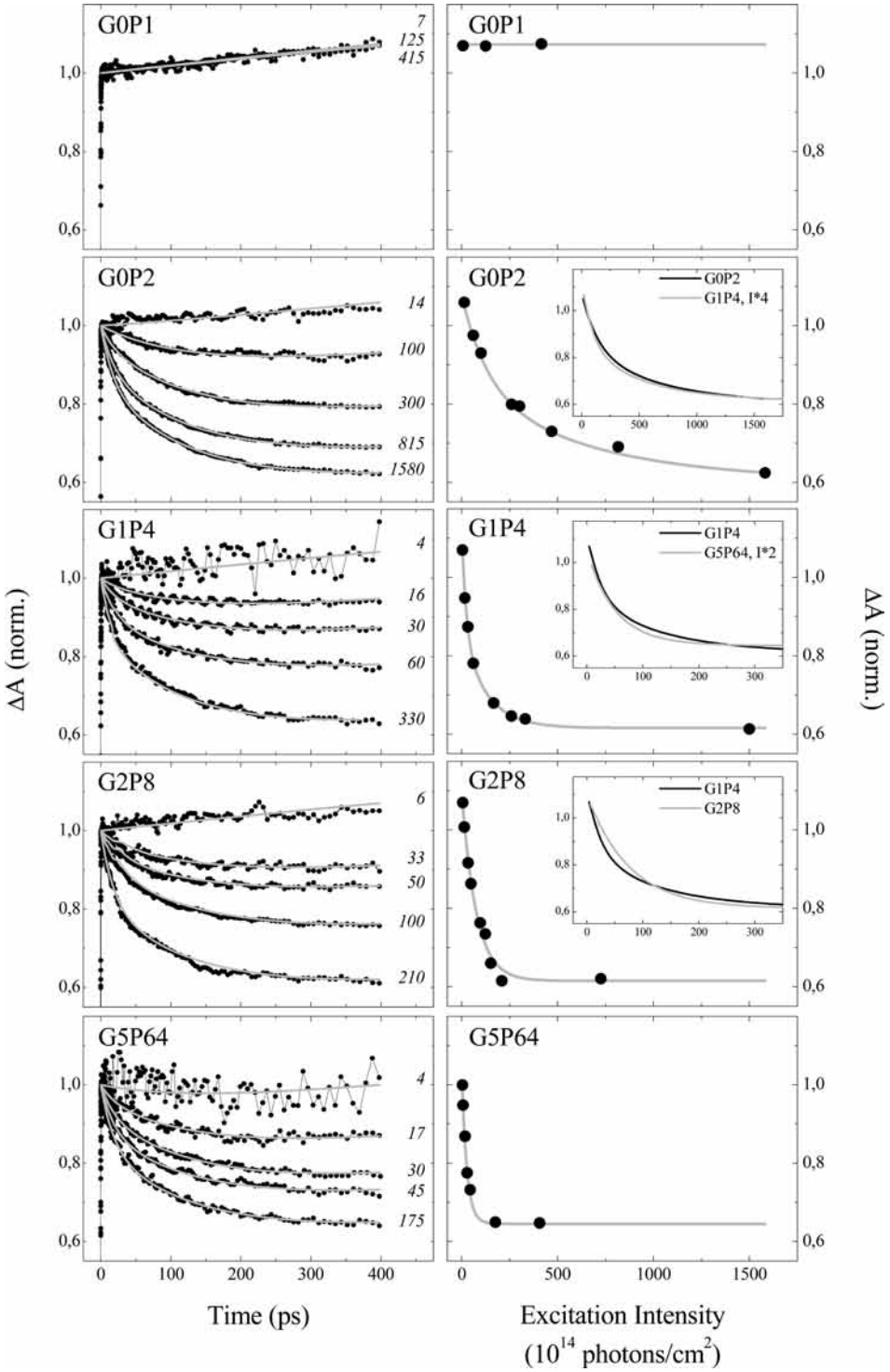

Figure 5. (left) Excitation intensity dependence of the compounds measured at 487 nm and normalized to unity at $t = 0$. The excitation intensities, $x \times 10^{14}$ photons/cm^2, are denoted next to the respective traces. The gray lines are the fits using eqs 7−11. (right) Measured ΔA value at $t = 400$ ps as a function of the excitation intensity is marked with circles, whereas the gray lines are double-exponential fits of the measurements merely meant as a guidance for the eye. The inset in the G0P2 window shows the guidance fit for G0P2 compared to the fit of G1P4, where the excitation intensity has been multiplied by a factor of 4. In the G1P4 window, the inset shows the guidance fits for G1P4 and G5P64 with the excitation intensity of G5P64 multiplied by a factor of 2. Likewise, the guidance fits for G1P4 and G2P8 are displayed in the inset in the G2P8 window (no multiplication of the excitation intensities).

population is observed, since one excited Zn-porphyrin is deexcited to the ground state. The amplitudes of the transient signals are accordingly decreased. At the 487 nm probing wavelength, the observed kinetics only has contributions from singlet excited state absorption and triplet absorption.

The transient absorption kinetics measured at different excitation intensities and afterward normalized at maximum signal are shown in Figure 5. The excitation intensities ($x \times 10^{14}$ photons/cm^2 per pulse) employed to obtain the individual kinetics are denoted next to the traces. No intensity dependence is observed for G0P1, which excludes excimer formation and aggregation. The transient signal increases as a function of time, which is attributed to the triplet formation, as the extinction coefficient for the triplet transition is larger than the extinction

coefficient of the transition from the S_1 state at 487 nm (see the Discussion section).

In contrast to G0P1, pronounced excitation intensity dependence is observed for G0P2 and the dendrimers. The transient kinetics measured at the lowest excitation intensity in G0P2, G1P4, and G2P8 resemble the G0P1 kinetics, and is therefore assigned to the triplet formation. Upon increase of the excitation intensity, similar multiexponential kinetics are observed in G0P2−G5P64. The kinetics can globally be described by two shorter time components of 18 ± 5 ps and 130 ± 10 ps and the slow (>1 ns) absorbance increase due to the triplet formation. Since neither of the two short time components is observed in G0P1, they are assigned to the singlet−singlet annihilation processes.

Depending on the size of the compound, different excitation intensities are required to get analogous kinetics. For G0P2, 4 times higher excitation intensities are needed to obtain the same kinetics as observed in G1P4. The excitation intensity dependence of G1P4 and G2P8 is comparable, whereas only half the excitation intensity is required to measure similar kinetics for the largest dendrimer, G5P64. At high excitation intensity, the transient kinetics of G0P2−G5P64 decay to a level of ∼55% of the signal measured in G0P1 at 400 ps. For G1P4 and G2P8, the plateau is reached at an excitation intensity of $\sim 225 \times 10^{14}$ photons/cm^2, whereas an excitation intensity of only $\sim 100 \times 10^{14}$ photons/cm^2 is needed in G5P64 (see the right side of Figure 5). Increasing the excitation intensity further does not decrease the transient signal in any of the compounds. Hence, the onset of the singlet−singlet annihilation and the excitation intensity required to reach the 55% plateau varies depending on the size of the compound.

4. Discussion

4.1. Dependence on the Dendrimer Size. The onset of the singlet−singlet annihilation processes varies with the size of the molecule, and the number of nearest-neighbor Zn-porphyrins therefore needs to be considered. In G1P4 there are three different nearest-neighbor Zn-porphyrins, whereas in G0P2 there is only one. The possibility of exciting a second Zn-porphyrin in G1P4 is therefore 3 times larger than in G0P2. Consequently, the onset of annihilation should occur at 3 times lower excitation intensity. This is in reasonable agreement with the measurements showing that approximately 4 times higher excitation intensity is required to obtain the same kinetics in G0P2 as observed in G1P4 and G2P8 (see the right side of Figure 5).

If all the Zn-porphyrins in G2P8 communicate, only half the excitation intensity would be needed to obtain the same kinetics as observed in G1P4. However, for G1P4 and G2P8 about the same excitation intensity dependence is observed. Accordingly, the Zn-porphyrins in G2P8 must be arranged in two separate dendron groups. In G5P64 only half the excitation intensity is required to obtain the same kinetics as observed for G1P4 and G2P8 (see the insets on the right side of Figure 5). The number of nearest-neighbor Zn-porphyrins is therefore six—twice that in the two smaller dendrimers. Taking into account the higher density of Zn-porphyrins on the molecular surface of G5P64, this is a very reasonable scenario. The singlet−singlet annihilation processes can therefore occur with three other Zn-porphyrins within a dendron for G1P4 and G2P8 and with six nearest-neighbor Zn-porphyrins in G5P64.

4.2. Assignment of the Two Singlet−Singlet Annihilation Time Constants. The observed annihilation processes could in principle originate from both singlet−triplet annihilation and singlet−singlet annihilation. However, since the spectral overlap between the triplet (T_1) absorption spectrum and the S_1 emission spectrum is very poor compared to the spectral overlap between the S_1 emission spectrum and the S_1 absorption spectrum, the annihilation process is assigned to singlet−singlet annihilation. Further, the probability of observing singlet−triplet annihilation is reduced due to the use of a rotational cuvette in all the measurements. To reproduce the singlet−singlet annihilation kinetics displayed in Figure 5, eqs 7−11 have been utilized. For the monomer, no annihilation can occur and eq 7 reduces to a single exponential. Using the S_1 lifetime of 2.7 ns and the ISC yield of 84% (hence $k_{ISC} = 3.2$ ns) measured by Rogers et al. for a very similar compound,[51] the only unknown is the ratio p between the extinction coefficient of the S_1 state transition and the triplet transition at the selected probe wavelength. From the fits of the G0P1 kinetics measured at three different excitation intensities, an average of $p = 1.8$ is established. Due to the similarities of the transient spectra of all the compounds, $p = 1.8$ is used in each of the fits. The two annihilation time constants, $\tau_f = 18 \pm 5$ ps and $\tau_s = 130 \pm 10$ ps, are obtained by global fitting. Since the same annihilation time constants are found in G0P2−G5P64, both processes can be described using the annihilation theory developed in section 2.1 for G0P2.

Previously, observation of two distinct singlet−singlet annihilation time constants has been reported in polyphenyl dendrimers[23] and porphyrin boxes.[40] In both studies, the two time constants were explained by annihilation between two sets of chromophores arranged at different distances. The two distinct time constants observed in the singlet−singlet annihilation kinetics for G0P2−G5P64 could be explained in the same way, since the distance between and the orientation of the individual Zn-porphyrins within the dendrimer can vary. Note that the Zn-porphyrin dendrimers are very flexible and there are therefore not two fixed distances, but distributions of different distances and dipole-moment orientations. It is thus reasonable to suggest that the two different structural conformer distributions give rise to the two annihilation time constants observed in G0P2. For the larger dendrimers, many more conformer distributions probably exist, but the observation of the same two annihilation time constants for G0P2−G5P64 shows that the four to seven Zn-porphyrins among which annihilation occur have intermolecular distances and orientations similar to those of the G0P2 dimer. For G1P4 and G2P8, this is not surprising considering the length and structure of the inter-porphyrin links in a dendron. The denser packing of Zn-porphyrins in G5P64 results in annihilation somewhat outside a dendron, involving another three Zn-porphyrins. The results show that, within the precision of multiexponential fitting, the same two annihilation time constants are obtained for G5P64 and the smaller dendrimers, suggesting similar distances and orientations among all the annihilating Zn-porphyrins of G5P64. Considering the inherent uncertainty in multiexponential fitting with possible tradeoff between amplitudes and lifetimes, it should be emphasized that the most important result of the present work is the variation in the number of interacting Zn-porphyrins with the size of the dendrimer, and the existence of distinguishable structural distributions. The fact that we are dealing with distributions of structural conformations implies that structural information is only qualitative.

Förster ET theory can without difficulty account for the two time components assuming that either (1) the dipole moments of the two Zn-porphyrins have different orientations, (2) the distance between the two Zn-porphyrins has two different equilibriums, or (3) a combination of (1) and (2). The presence of more than two conformer distributions cannot be excluded,

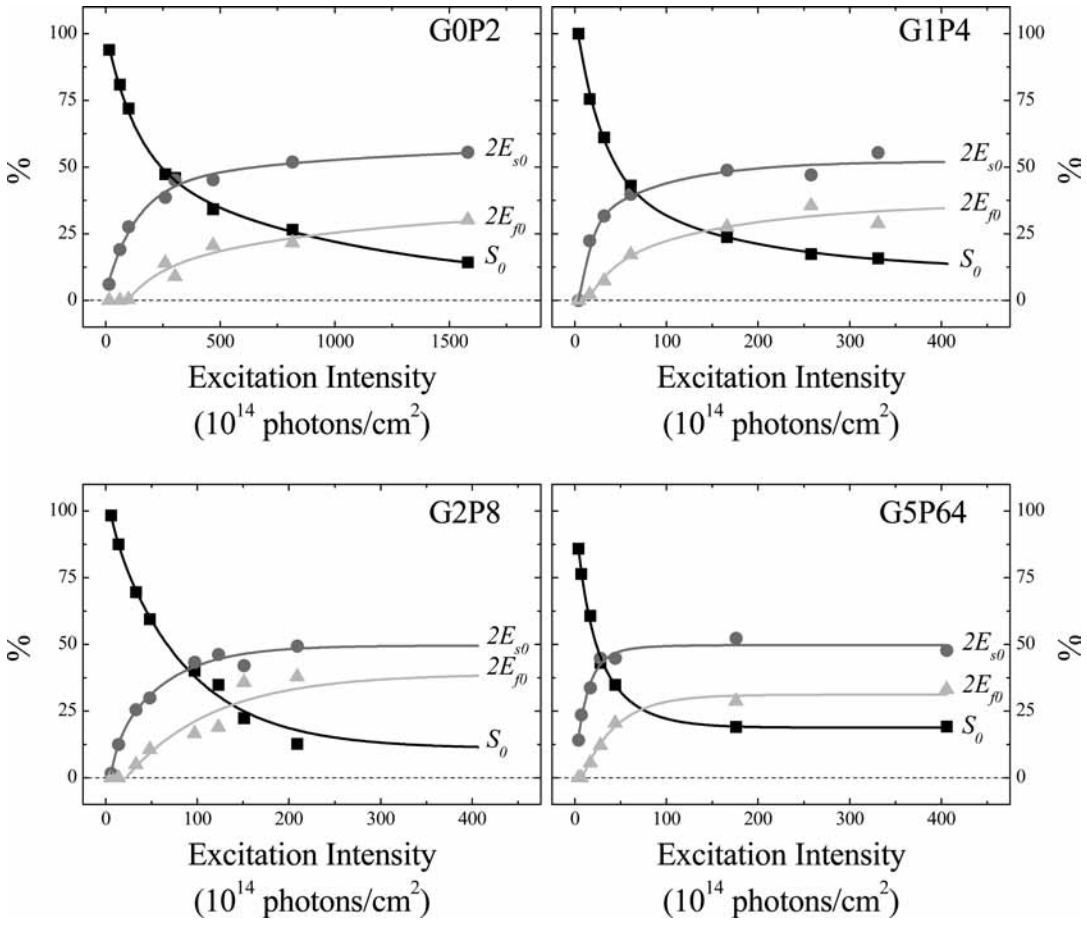

Figure 6. Amplitudes obtained from singlet−singlet annihilation fits with eqs 7−11 plotted in percent. The lines are double-exponential fits of the amplitudes and serve merely as guidance for the eye. The uncertainty is ±5%. Note that the excitation intensity scale is different for G0P2 compared to the other molecules.

as the observed kinetics can be described equally well by a multiexponential function using more than three exponentials.

Time-resolved fluorescence anisotropy measurements have previously demonstrated ET from an excited Zn-porphyrin to a nonexcited Zn-porphyrin occurring on a time scale of 100 ± 25 ps.[49] Förster ET theory utilized to model the ET process showed that the ET primarily occurs between the two nearest-neighbor Zn-porphyrins at a distance of 2 nm. In the fluorescence anisotropy measurements, the spectral overlap was between the emission spectrum of the donor and the absorption spectrum of the acceptor. The Förster ET process in singlet−singlet annihilation on the other hand requires a spectral overlap between the emission spectrum of the donor and the excited state spectrum of the acceptor. Subtracting the contribution from the ground state bleaching and the stimulated emission from the transient spectrum at 5 ps displayed in Figure 3 gives the excited state absorption spectrum. The spectrum has a maximum at 470 nm and a long tail extending beyond 700 nm. The dipole strength of the excited state transition and the spectral overlap between the excited state spectrum and the emission spectrum can be calculated from the estimated excited state absorption spectrum, where the approximate value of the extinction coefficient is obtained from comparison with the ground state bleaching. Based on this calculation, the singlet−singlet annihilation Förster ET process is expected to be approximately 4−8 times faster than the Förster ET measured in the time-resolved fluorescence anisotropy experiments, mainly due to the larger value of the spectral overlap integral. Since we have only measured the excited state spectrum between 450 and 730 nm, the Förster ET in singlet−singlet annihilation cannot be determined with higher accuracy. The singlet−singlet annihilation time constant of $\tau_f = 18 \pm 5$ ps is 5 times faster than the Förster ET time constant of 100 ± 25 ps observed in the fluorescence anisotropy measurements.[49] This difference in ET rates is in agreement with the estimates above, and we therefore conclude that the fast annihilation process and the ET process observed in the anisotropy measurements originate from the same structural conformer disribution. The counterpart to the slow annihilation time constant of $\tau_s = 130 \pm 10$ ps would have been on the order of ∼1 ns in the fluorescence anisotropy measurements. This time component could not be observed because it was impossible to separate it from the rotational time constant of 1.7 ns. However, it is worth mentioning that in the free-base version of the Zn-porphyrin dendrimers presented here, a similar ET component on a nanosecond time scale has been observed at 77 K.[29]

Figure 6 shows the amplitudes, S_0, E_{f0}, and E_{s0} (plotted in percent), that are obtained from the singlet−singlet annihilation fits using eq 7. The annihilation amplitudes, E_{f0} and E_{s0}, each represent the excitation of two Zn-porphyrins and are thus multiplied by a factor of 2. When on average half of the Zn-porphyrins in G1P4 are excited, 12.5% of the molecules will only be singly excited. This is in very good agreement with the observation at high excitation intensities, where the percentage of excited molecules that are not involved in the annihilation process (S_0) drops to 10−15%. Additionally, at high excitation intensities, the amplitude ratio between the fast and slow annihilation components is approximately 1:2, demonstrating

that the structural conformer distribution connected to the slow annihilation component is the dominating one.

4.3. Sequential Annihilation within the Dendrimers. According to the Einstein coefficients for absorption and stimulated emission, upon excitation the probability of absorption and of stimulated emission is the same in a two-level system. The lifetime of the S_2 state into which we excite is ~1 ps, and the system can thus be approximated by a two-level system within the time duration of the excitation pulse. On average a maximum of 50% of the chromophores can consequently be excited. For G1P4 this implies that more than two Zn-porphyrins will be excited in ~30% of the dendrimers. Since annihilation can take place between all the Zn-porphyrins, two extra exponentials for each of the structural conformer distributions—one representing excitation of three Zn-porphyrins and one for excitation of four Zn-porphyrins—need to be added.[47] Hence, a total of four additional exponentials need to be included. The ratio between the rate constants for annihilation in G1P4 with two, three, or four excited Zn-porphyrins is 1:3:6,[47] reflecting the number of possible annihilation processes. Introducing the four extra components in eq 7 only improves the fit to a minor extent, as the amplitudes of the additional components are small. The data can therefore be adequately described with the two-exciton annihilation theory. Including only one structural conformer distribution yields a poor fit of the data, due to the restriction of the ratio between the annihilation rates. Hence, at least two different structural conformer distributions are required to explain the data.

In the dendrimers, where more than two of the Zn-porphyrins are excited, annihilation involving the same chromophore can occur two or three times depending on whether three or four Zn-porphyrins are excited, respectively. This process is referred to as sequential annihilation. If on average 50% of the Zn-porphyrins in G1P4 are excited and sequential annihilation occurs, the transient signals will decrease to approximately 50% of the monomer signal. This matches well with the observations of the 55% plateau in G1P4 (see Figure 5). To obtain the observed 55 % without including sequential annihilation requires excitation of nearly all the Zn-porphyrins, which obviously seems unrealistic. The similarity in the excitation intensity dependence of G1P4 and G2P8 shows that G2P8 can be viewed as two dendron units. Excitation of 50% of the Zn-porphyrins in G2P8 should therefore yield kinetics similar to that for G1P4, in good agreement with the observations.

In G5P64, annihilation can occur to six Zn-porphyrins. However, the distances between all the chromophores in the unit of seven annihilating Zn-porphyrins in G5P64 are not the same, and G5P64 cannot be viewed as subunits of seven fully communicating Zn-porphyrins. Therefore, in order for sequential annihilation to occur between all seven Zn-porphyrins in the G5P64 subunit, one or more ET steps from an excited to an unexcited Zn-porphyrin will be required in a number of cases. ET occurs on a ~100 ps time scale if the units are situated close to one another separated by a distance of ~2 nm (a random orientation of the dipoles is assumed).[49] However, if the distances between the Zn-porphyrins are on the order of 3 nm or longer, the ET will be too slow (>1 ns) to be observed on the 400 ps time scale.[49] Since the structural conformer distribution connected to the slow annihilation time component is the dominating one (see Figure 6) and this annihilation time corresponds to an ET time of ~1 ns, it is not likely that sequential annihilation occurring after ET will show up on the reported time scale. Assuming an average excitation of 50% of the Zn-porphyrins and at the same time excluding contributions from sequential annihilation after ET, the kinetics for G5P64 is expected to decay to a plateau of ~40%. This is lower than the observed level at ~55%, which suggests that either (1) direct sequential annihilation (i.e., without ET to unexcited Zn-porphyrins) is not present in all the cases where it is statistically possible, or (2) less than 50% of the Zn-porphyrins are excited. Due to the high value of the maximum excitation intensity, the latter explanation is less likely.

In G0P2, sequential annihilation is not possible, since there are only two Zn-porphyrins. If half of the Zn-porphyrins in G0P2 are excited, 25% of the molecules will be doubly excited. Singlet−singlet annihilation should accordingly reduce the transient signal to 75% compared to the monomer signal at 400 ps. Half the Zn-porphyrins in G1P4 are excited at an excitation intensity of 225×10^{14} photons/cm^2 per pulse, as the 55% plateau is observed above this excitation intensity (see Figure 5). In G0P2 a decay to ~75% is observed at this excitation intensity, corresponding very well to the expectations. Excitation intensities above 225×10^{14} photons/cm^2 per pulse do not result in a lower plateau for G1P4−G5P64, in agreement with the assumption that the system upon excitation can be approximated by a two-level system. However, for G0P2 a plateau below the expected 75% is observed at very high excitation intensities (above 225×10^{14} photons/cm^2 per pulse). Preliminary simulations have shown that it is possible to coherently excite more than half the Zn-porphyrins in G0P2 within the duration of the excitation pulse, thereby providing a possible explaination of the lower plateau at 55%. If it also is possible to coherently excite more than an average of 50% of the Zn-porphyrins in the larger dendrimers, sequential annihilation needs to be less pronounced than is assumed here. Further work on this is in progress.[52]

5. Conclusion

In this article, we have studied the singlet−singlet annihilation within a series of Zn-porphyrin dendrimers by means of intensity dependent transient absorption experiments. Two singlet−singlet annihilation processes are observed in the G0P2−G5P64 dendrimers: a slow annihilation of 130 ± 10 ps and a fast annihilation of 18 ± 5 ps. Both annihilation processes can be well described with Förster ET theory. The origin of two distinct time components is a result of different conformational distributions of the Zn-porphyrins within the dendrimers. The amplitude of the slower component is a factor of 2 larger than the amplitude of the faster component.

The onset of the annihilation is different depending on the size of the molecule. The excitation intensity dependence adequately reflects the variation in the number of nearest-neighbor Zn-porphyrins with which annihilation can occur. In G1P4 and G2P8, annihilation can take place with the three nearest-neighbor Zn-porphyrins. G2P8 can consequently be viewed as two separate dendron units. In G5P64 annihilation can occur with six nearest-neighbor Zn-porphyrins, showing that, in the largest dendrimer, interactions extend outside the dendron unit of four Zn-porphyrins.

The kinetics of G0P2−G5P64 approach a lower plateau of ~55% compared to the monomer at high excitation intensities. This plateau value shows that sequential annihilation is present in G1P4−G5P64, when on average half the Zn-porphyrins are excited. For the dimer, the plateau value implies that more than half the Zn-porphyrins must be excited. Additional simulations have been initiated to investigate coherent excitation within the excitation pulse, which can yield excitation of more than 50% of the Zn-porphyrins.

Acknowledgment. Financial support from the Swedish Research Council, the Swedish Energy Agency, the Knut and Alice Wallenberg Foundation, and the Magnus Bergwall Foundation is gratefully acknowledged. We further thank the Australian Research Council for a Discovery Research Grant (DP0208776) to M.J.C. Experimental assistance from Dr. Han-Kwang Nienhyus and valuable discussion with Dr. Tõnu Pullerits and Dr. Johan Andersson are highly appreciated.

References and Notes

(1) Jansen, J. F. G. A.; de Brabander-van den Berg, E. M. M.; Meijer, E. W. *Science* **1994**, *266*, 1226.

(2) Matthews, O. A.; Shipway, A. N.; Stoddart, J. F. *Prog. Polym. Sci.* **1998**, *23*, 1.

(3) Brousmiche, D. W.; Serin, J. M.; Fréchet, J. M. J.; He, G. S.; Lin, T. C.; Chung, S. J.; Prasad, P. N. *J. Am. Chem. Soc.* **2003**, *125*, 1448.

(4) Ghaddar, T. H.; Wishart, J. F.; Thompson, D. W.; Whitesell, J. K.; Fox, M. A. *J. Am. Chem. Soc.* **2002**, *124*, 8285.

(5) Pollak, K. W.; Leon, J. W.; Fréchet, J. M. J.; Maskus, M.; Abruña, H. D. *Chem. Mater.* **1998**, *10*, 30.

(6) Bar-Haim, A.; Klafter, J.; Kopelman, R. *J. Am. Chem. Soc.* **1997**, *119*, 6197.

(7) Bar-Haim, A.; Klafter, J. *J. Phys. Chem. B* **1998**, *102*, 1662.

(8) Betley, T. A.; Holl, M. M. B.; Orr, B. G.; Swanson, D. R.; Tomalia, D. A.; Baker, J. R. *Langmuir* **2001**, *17*, 2768.

(9) Bielinska, A.; Kukowska-Latallo, J. F.; Johnson, J.; Tomalia, D. A.; Baker, J. R. *Nucleic Acids Res.* **1996**, *24*, 2176.

(10) Ottaviani, M. F.; Sacchi, B.; Turro, N. J.; Chen, W.; Jockusch, S.; Tomalia, D. A. *Macromolecules* **1999**, *32*, 2275.

(11) Roberts, J. C.; Bhalgat, M. K.; Zera, R. T. *J. Biomed. Mater. Res.* **1996**, *30*, 53.

(12) Singh, P. *Bioconjugate Chem.* **1998**, *9*, 54.

(13) Tomalia, D. A. *Sci. Am.* **1995**, *272*, 62.

(14) Twyman, L. J.; Beezer, A. E.; Esfand, R.; Hardy, M. J.; Mitchell, J. C. *Tetrahedron Lett.* **1999**, *40*, 1743.

(15) Andersson, J.; Puntoriero, F.; Serroni, S.; Yartsev, A.; Pascher, T.; Polivka, T.; Campagna, S.; Sundström, V. *Faraday Discuss.* **2004**, *127*, 295.

(16) Andersson, J.; Puntoriero, F.; Serroni, S.; Yartsev, A.; Pascher, T.; Polivka, T.; Campagna, S.; Sundström, V. *Chem. Phys. Lett.* **2004**, *386*, 336.

(17) Balzani, V.; Campagna, S.; Denti, G.; Juris, A.; Serroni, S.; Venturi, M. *Acc. Chem. Res.* **1998**, *31*, 26.

(18) Choi, M. S.; Aida, T.; Yamazaki, T.; Yamazaki, I. *Chem.—Eur. J.* **2002**, *8*, 2668.

(19) De Belder, G.; Jordens, S.; Lor, M.; Schweitzer, G.; De, R.; Weil, T.; Herrmann, A.; Wiesler, U. K.; Müllen, K.; De Schryver, F. C. *J. Photochem. Photobiol. A: Chem.* **2001**, *145*, 61.

(20) Fleming, C. N.; Maxwell, K. A.; DeSimone, J. M.; Meyer, T. J.; Papanikolas, J. M. *J. Am. Chem. Soc.* **2001**, *123*, 10336.

(21) Karni, Y.; Jordens, S.; De Belder, G.; Hofkens, J.; Schweitzer, G.; De Schryver, F. C.; Herrmann, A.; Müllen, K. *J. Phys. Chem. B* **1999**, *103*, 9378.

(22) Lor, M.; Thielemans, J.; Viaene, L.; Cotlet, M.; Hofkens, J.; Weil, T.; Hampel, C.; Müllen, K.; Verhoeven, J. W.; Van der Auweraer, M.; De Schryver, F. C. *J. Am. Chem. Soc.* **2002**, *124*, 9918.

(23) Lor, M.; De, R.; Jordens, S.; De Belder, G.; Schweitzer, G.; Cotlet, M.; Hofkens, J.; Weil, T.; Herrmann, A.; Müllen, K.; Van der Auweraer, M.; De Schryver, F. C. *J. Phys. Chem. A* **2002**, *106*, 2083.

(24) Hofkens, J.; Latterini, L.; De Belder, G.; Gensch, T.; Maus, M.; Vosch, T.; Karni, Y.; Schweitzer, G.; De Schryver, F. C.; Hermann, A.; Müllen, K. *Chem. Phys. Lett.* **1999**, *304*, 1.

(25) Schweitzer, G.; Gronheid, R.; Jordens, S.; Lor, M.; De Belder, G.; Weil, T.; Reuther, E.; Müllen, K.; De Schryver, F. C. *J. Phys. Chem. A* **2003**, *107*, 3199.

(26) Karni, Y.; Jordens, S.; De Belder, G.; Schweitzer, G.; Hofkens, J.; Gensch, T.; Maus, M.; De Schryver, F. C.; Hermann, A.; Müllen, K. *Chem. Phys. Lett.* **1999**, *310*, 73.

(27) Maus, M.; De, R.; Lor, M.; Weil, T.; Mitra, S.; Wiesler, U. M.; Herrmann, A.; Hofkens, J.; Vosch, T.; Müllen, K.; De Schryver, F. C. *J. Am. Chem. Soc.* **2001**, *123*, 7668.

(28) Maus, M.; Mitra, S.; Lor, M.; Hofkens, J.; Weil, T.; Herrmann, A.; Müllen, K.; De Schryver, F. C. *J. Phys. Chem. A* **2001**, *105*, 3961.

(29) Yeow, E. K. L.; Ghiggino, K. P.; Reek, J. N. H.; Crossley, M. J.; Bosman, A. W.; Schenning, A. P. H. J.; Meijer, E. W. *J. Phys. Chem. B* **2000**, *104*, 2596.

(30) Yatskou, M. M.; Koehorst, R. B. M.; van Hoek, A.; Donker, H.; Schaafsma, T. J. *J. Phys. Chem. A* **2001**, *105*, 11432.

(31) Ferreira, K. N.; Iverson, T. M.; Maghlaoui, K.; Barber, J.; Iwata, S. *Science* **2004**, *303*, 1831.

(32) Jordan, P.; Fromme, P.; Witt, H. T.; Klukas, O.; Saenger, W.; Krauss, N. *Nature* **2001**, *411*, 909.

(33) Roszak, A. W.; Howard, T. D.; Southall, J.; Gardiner, A. T.; Law, C. J.; Isaacs, N. W.; Cogdell, R. J. *Science* **2003**, *302*, 1969.

(34) Papiz, M. Z.; Prince, S. M.; Howard, T.; Cogdell, R. J.; Isaacs, N. W. *J. Mol. Biol.* **2003**, *326*, 1523.

(35) Camara-Artigas, A.; Blankenship, R. E.; Allen, J. P. *Photosynth. Res.* **2003**, *75*, 49.

(36) Tronrud, D. E.; Matthews, B. W. In *Photosynthetic Reaction Center*; Deisenhofer, J., Norris, J. R., Eds.; Academic Press: New York, 1993.

(37) Sundström, V.; Pullerits, T.; van Grondelle, R. *J. Phys. Chem. B* **1999**, *103*, 2327.

(38) Yeow, E. K. L.; Sintic, P. J.; Cabral, N. M.; Reek, J. N. H.; Crossley, M. J.; Ghiggino, K. P. *Phys. Chem. Chem. Phys.* **2000**, *2*, 4281.

(39) Varnavski, O.; Samuel, I. D. W.; Pålsson, L. O.; Beavington, R.; Burn, P. L.; Goodson, T. *J. Chem. Phys.* **2002**, *116*, 8893.

(40) Hwang, I.-W.; Kamada, T.; Ahn, T. K.; Ko, D. M.; Nakamura, T.; Tsuda, A.; Osuka, A.; Kim, D. *J. Am. Chem. Soc.* **2004**, *126*, 16187.

(41) Jordens, S.; De Belder, G.; Lor, M.; Schweitzer, G.; Van der Auweraer, M.; Weil, T.; Herrmann, A.; Wiesler, U. M.; Müllen, K.; De Schryver, F. C. *Photochem. Photobiol. Sci.* **2003**, *2*, 1118.

(42) Brüggemann, B.; Herek, J. L.; Sundström, V.; Pullerits, T.; May, V. *J. Phys. Chem. B* **2001**, *105*, 11391.

(43) Trinkunas, G.; Herek, J. L.; Polívka, T.; Sundström, V.; Pullerits, T. *Phys. Rev. Lett.* **2001**, *86*, 4167.

(44) Brüggemann, B.; May, V. *J. Chem. Phys.* **2004**, *120*, 2325.

(45) Gulbinas, V.; Valkunas, L.; Kuciauskas, D.; Katilius, E.; Liuolia, V.; Zhou, W. L.; Blankenship, R. E. *J. Phys. Chem.* **1996**, *100*, 17950.

(46) Valkunas, L.; Åkesson, E.; Pullerits, T.; Sundström, V. *Biophys. J.* **1996**, *70*, 2373.

(47) van Amerongen, H.; Valkunas, L.; van Grondelle, R. *Photosynthetic excitons*; World Scientific Publishing: Singapore, 2000.

(48) Larsen, J.; Andersson, J.; Polívka, T.; Sly, J.; Crossley, M. J.; Sundström, V.; Åkesson, E. *Femtochemistry and Femtobiology*; Elsevier: 2004; 495−498.

(49) Larsen, J.; Andersson, J.; Polívka, T.; Sly, J.; Crossley, M. J.; Sundström, V.; Åkesson, E. *Chem. Phys. Lett.* **2005**, *403*, 205.

(50) Sly, J. Ph.D. Thesis, The University of Sydney, 2004.

(51) Rogers, J. E.; Nguyen, K. A.; Hufnagle, D. C.; McLean, D. G.; Su, W. J.; Gossett, K. M.; Burke, A. R.; Vinogradov, S. A.; Pachter, R.; Fleitz, P. A. *J. Phys. Chem. A* **2003**, *107*, 11331.

(52) Brüggemann, B.; Larsen, J.; Polívka, T.; Sundström, V.; Åkesson, E.; Pullerits, T. Manuscript in preparation.